

SCIENTIFIC REPORTS



OPEN

Fragmentation transitions in a coevolving nonlinear voter model

Byungjoon Min & Maxi San Miguel

We study a coevolving nonlinear voter model describing the coupled evolution of the states of the nodes and the network topology. Nonlinearity of the interaction is measured by a parameter q . The network topology changes by rewiring links at a rate p . By analytical and numerical analysis we obtain a phase diagram in p, q parameter space with three different phases: Dynamically active coexistence phase in a single component network, absorbing consensus phase in a single component network, and absorbing phase in a fragmented network. For finite systems the active phase has a lifetime that grows exponentially with system size, at variance with the similar phase for the linear voter model that has a lifetime proportional to system size. We find three transition lines that meet at the point of the fragmentation transition of the linear voter model. A first transition line corresponds to a continuous absorbing transition between the active and fragmented phases. The other two transition lines are discontinuous transitions fundamentally different from the transition of the linear voter model. One is a fragmentation transition between the consensus and fragmented phases, and the other is an absorbing transition in a single component network between the active and consensus phases.

The structure of networks on which interactions between individuals take place affects the dynamical processes between agents^{1,2}. At the same time, the pattern of social ties constantly changes under the strong influence of the state of individuals^{3–6}. Coevolution of individual states and network structures⁷ in a comparable time scale is commonly observed in reality^{8,9}. For example, individuals who are connected on a given network may become alike since they interact with each other via an existing social tie. At the same time social connections can also be established between people because they have some similarity⁴. In order to model the coevolutionary dynamics, there have been several attempts combining dynamics on top of networks and evolution of networks according to the state of individuals in different contexts of game theory^{10–14}, opinion formation^{15–18}, and epidemic dynamics^{19–21} among other. One of the simplest yet fruitful models is a coevolving voter model, describing the change of the state of the nodes following the rule of the voter model dynamics and organization of a network by rewiring links^{15,17,22–28}. The coevolving voter model exhibits a fragmentation transition from a single connected network to a network with two components^{15,17}.

In the original voter model, a voter (a node of the network) can be in either of two discrete states and it imitates the state of one of its neighbors chosen randomly. This simple rule implies a dyadic interaction in which the state of the majority of the neighbors does not play a role other than in an average manner. However, several neighbors can influence collectively an individual's state so that an agent may consider the state of more than one neighbor to change its state, rather than blindly copying the state of one of its random neighbors. This implies a nonlinear interaction of an agent with its neighborhood implemented as a nonlinear voter model^{29,30}. Conceptually, the difference between the ordinary voter model and the nonlinear voter model is the same discussed for simple and complex contagion processes^{31,32}. The same form of nonlinear interaction with the neighborhood of the nonlinear voter model is the one considered to model social pressure in social impact theory³³ as well as in language competition dynamics, named volatility^{34,35}, or in language evolution problems³⁶.

In this paper, we study the role of nonlinearity in a coevolving voter model by combining evolutionary dynamics of networks and a nonlinear voter model characterized by a degree of nonlinearity q . To be specific, we update the state or the links of node i in the network with a probability ρ_i^q where ρ_i is the fraction of neighbors of i in a different state than i . Mathematically ρ_i is defined as $(a_i)/(k_i)$ where k_i is the total number of neighbors called the degree of i and a_i is the number of active links connecting i to a node in a different state. When q is larger than 1, an agent follows the majority opinion more frequently than in the ordinary voter model. By contrast, minority opinion of neighbors is more likely to be chosen than in the linear model when q is less than 1. When the

IFISC, Instituto de Física Interdisciplinar y Sistemas Complejos (CSIC-UIB), Campus Universitat Illes Balears, E-07122, Palma, Spain. Correspondence and requests for materials should be addressed to B.M. (email: byungjoon@ifisc.uib-csic.es) or M.S.M. (email: maxi@ifisc.uib-csic.es)

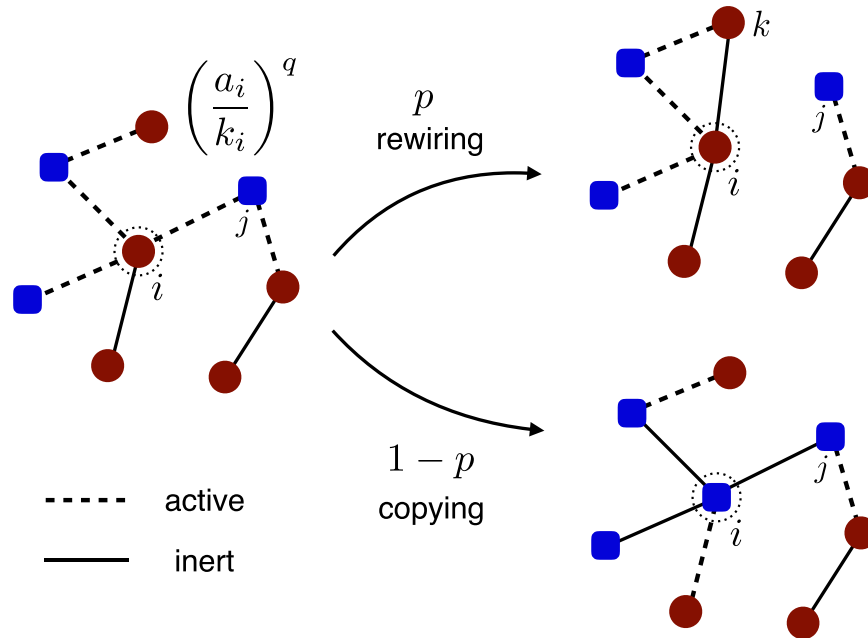


Figure 1. Schematic illustration of update rule of the coevolving nonlinear voter model. Each node is in either up (red circle) or down (blue rounded square) state. Solid and dashed lines indicate respectively inert and active links. At each step, we randomly choose a node i . And we choose one of its neighbors j connected by an active link with a probability $((a_i)/(k_i))^q$. Then, we rewire an active link with a probability p and copy the state of the neighbor with a probability $1 - p$.

parameter q takes integer values, it can be interpreted as a voter selecting multiple neighbors and changing its state when all selected neighbors have unanimously a different state²⁹. However, q is taken as a continuous parameter in social impact theory or in language evolution dynamics. While it is argued that $q < 1$ in social impact theory³³ and language evolution³⁶, it was fitted to $q = 1.3$ to account for data on different language extinction processes³⁴. We study the role of nonlinearity measured by q in the fragmentation transition of the voter model: We find that the coevolving nonlinear voter model still shows a fragmentation transition between connected and disconnected networks but with different mechanisms depending on the nonlinearity q . For $q < 1$ the system undergoes a continuous transition between a dynamically active phase and an absorbing frozen state with two disconnected clusters each of them in a different consensus state, i.e. in each cluster all the nodes are in the same state, but this state is different in both clusters. This is the same transition found for the ordinary voter model ($q = 1$) in the thermodynamic limit $N \rightarrow \infty$. However, for finite but large systems $N \gg 1$ the coevolving linear voter model, $q = 1$, reaches a frozen state either in a fully consensus or a fragmented phase while the nonlinear coevolving model with $q < 1$ can remain in a dynamically active phase for observation times that grow exponentially with N . However, for $q > 1$ the transition is abrupt and between two absorbing states, therefore essentially different than the continuous transition observed in the ordinary voter model.

Results

Coevolving nonlinear voter model. We consider a degree regular network in which each node has the same number $\langle k \rangle$ of random neighbors. Each node i is initially either in a state $s_i = +1$ (up) or -1 (down) with the same probability $1/2$. In a given configuration, each link can be classified into two different types, active or inert. We define active (inert) links for the links connecting two nodes in different (same) states. We also define the density of active links ρ_i for each node i as $(a_i)/(k_i)$ where k_i is the degree and a_i is the number of active links of node i . At each step, we randomly choose a node i . And with a probability ρ_i^q , we choose at random an active link to a neighbor, say j . Note that with the complementary probability $1 - \rho_i^q$, nothing happens and we pick another node randomly. Once we choose node i and j , with a probability p node i removes the link to j and rewires a link to another node, say l , having the same state with i . And with a probability $1 - p$, node i flips its state to become the same as the state of node j (see Fig. 1). This proceeds, keeping the average degree $\langle k \rangle$ constant, until the system reaches a dynamically active steady state or an absorbing configuration.

The probability p , or plasticity parameter, represents a ratio of the time scale of evolution of the network and the time scale of evolution of the states of the nodes. When $p = 0$, the model corresponds to a nonlinear voter model on a static network. In contrast, for $p = 1$, the model describes a rewiring process to become two differently ordered groups. The degree of nonlinearity q controls the frequency of the selection of agents for execution. When $q > 1$, nodes with more active links have a higher chance to be changed than the ordinary voter model. In contrast, if $q < 1$, nodes with less active links are more likely to be changed. The model becomes the original voter model when $q = 1$.

Coexistence, consensus, and fragmented phases. The magnetization defined as $m = (1/N) \sum_i s_i$ and the density of active links ρ over a network satisfy coupled equations of evolution derived in a pair approximation in the Methods Section. The steady state solutions of these equations are: $(m, \rho) = (-1, 0), (1, 0), (0, \rho^*)$ and $(m^*, 0)$. The solutions $(-1, 0)$ and $(1, 0)$ represent a consensus absorbing frozen phase with all nodes in the same state. In contrast, $(0, \rho^*)$ indicates a dynamically active phase with coexistence of the same number of nodes in the up and down states where ρ^* represents the density of active links of the active phase. For the steady state solution with $m = 0$, the equation of ρ (Eq. 7) reduces to

$$\rho^q \{ -p + (1-p)(\langle k \rangle - 2q - 2(k-q)\rho) \} = 0, \quad (1)$$

and ρ^* is obtained as

$$\rho^* = \frac{(1-p)(\langle k \rangle - 2q) - p}{2(1-p)(\langle k \rangle - q)}. \quad (2)$$

Note that when $q = 1$, we recover the result for the coevolving linear voter model¹⁷, $\rho = ((1-p)(\langle k \rangle - 1) - 1) / (2(1-p)(\langle k \rangle - 1))$. Finally, the $(m^*, 0)$ solution corresponds to a fragmentation of the network in two components, each of them separately ordered. In general m^* is determined by the initial fraction of up and down nodes and in particular $m^* = 0$ for our initial condition $m = 0$. For different initial conditions, i.e. $m \neq 0$, the fragmented components can have different sizes. Note that solutions with $\rho = 0$ correspond to absorbing states in which the dynamics is frozen, including the fragmented phase $(m^*, 0)$.

In summary, there are three different types of stationary solutions with the initial condition $m = 0$: (i) $(m, \rho) = (0, \rho^*)$ corresponding to a dynamically active phase of coexistence in a single component network, (ii) $(-1, 0)$ or $(1, 0)$ which are consensus absorbing phases in a single component network, and (iii) $(0, 0)$ corresponding to an absorbing fragmented phase with a network composed of two disconnected clusters.

When $p = 0$, that is a nonlinear voter model on static networks, Eqs 6 and 7 have three sets of solutions, $(-1, 0)$, $(1, 0)$, and $(0, \rho^*)$, while the solution $(0, 0)$ corresponding to a fragmentation solution exists for $p \neq 0$. For small values of p , $(0, 0)$ is unstable, becoming stable by increasing p at a point p_c where $\rho^* = 0$ in Eq. 2. Explicitly, the transition point is given by $p_c = (\langle k \rangle - 2q) / (1 + \langle k \rangle - 2q)$ in the pair approximation. When $p > p_c$, the fragmented phase $(0, 0)$ is stable solution for all value of q . When $p < p_c$, the system is found in the dynamically active or absorbing phase in a single component network depending on the stability of the solution $(0, \rho^*)$ which is determined by the slope of Eq. 6 at a given q . If $q < 1$, the solution $(0, \rho^*)$ is stable, so the dynamically active phase is predicted. But when $q > 1$, the solution becomes unstable and $(-1, 0)$ and $(1, 0)$ are stable, so that the absorbing consensus phase is predicted.

In Fig. 2, the dynamical flow on the plane (m, ρ) to stable fixed points and the stability of them predicted from Eqs 6 and 7 are depicted. The system evolves by following the flow from initial state and eventually reaches stable fixed points (filled circle) or $\rho = 0$ line corresponding to an absorbing phase. For the case $q = 0.5$, when $p < p_c$, ρ^* at $m = 0$ is stable indicating coexistence of the two possible states of the nodes in a single connected network. The value of the number of active links ρ^* in the stable point gradually decreases with increasing p and becomes zero at p_c . When $p > p_c$ and for the initial condition $m = 0$, the system eventually arrives at the absorbing state $\rho = 0$ and $m = 0$ implying a network with two disconnected clusters with a different consensus in each of the clusters. Therefore, the mean-field analysis predicts a continuous transition between the active phase $(m, \rho) = (0, \rho^*)$ and an absorbing phase with two split clusters $(0, 0)$.

However, when $q = 2$, the stable fixed points are located at $(-1, 0)$ and $(1, 0)$ and the solution at $m = 0$ is unstable for $p < p_c$. Above p_c , $\rho = 0$ and $m = 0$ (for initial condition $m = 0$) is the steady state corresponding to the absorbing phase with a fragmented network. Therefore, at the transition the magnetization drops abruptly to be zero at p_c in a discontinuous transition. Thus we predict different phase transitions depending on q , that is a continuous phase transition from an active to a frozen absorbing state for $q \leq 1$ and a discontinuous transition between two absorbing states for $q > 1$.

Numerical results and finite-size analysis. In order to examine the different mechanisms of the fragmentation transition, we numerically measure the size of the largest component S , absolute value of magnetization $|m|$, and the density of active links for the network ρ^* at the steady state for $q = 0.5, 1$, and 2 (Fig. 3). The fragmented states above p_c for the three values of q share the common feature characterized by $(S, m, \rho^*) \approx (0.5, 0, 0)$, indicating a network with two disconnected clusters each of them in a different consensus state.

Below p_c , the network is in a single connected component regardless of the value of q but differently characterized by $(1, 0, \rho_{0.5}^*)$ for $q = 0.5$, $(1, 1, \rho_1^*)$ for $q = 1$, and $(1, 1, 0)$ for $q = 2$, where ρ^* is a non-zero value. For $q = 0.5$, the network forms a single component with a certain fraction of active links meaning that up and down states coexist. So, the system, in the thermodynamic limit, remains in a dynamically active state and does not reach the absorbing state. The value shown for ρ^* corresponds to the one in this thermodynamic limit and it is measured numerically as the density of active links averaged over surviving runs. On the contrary, when $q > 1$, the system reaches the consensus phase showing all nodes are in the same state within a single component. For $q = 1$ which is the linear coevolving voter model, the active state is observed by showing non-zero ρ^* as expected in the analytic prediction, Eqs 6 and 7. ρ^* is again calculated averaging only over surviving runs. However, due to finite size fluctuations the system goes to an absorbing consensus phase below p_c ¹⁷ showing $m = 1$ in Fig. 3(b).

In the right panels in Fig. 3, a typical trajectory on (m, ρ) space also exhibits different mechanisms to approach the steady state depending on the value of q . Red symbols (\square) for $q = 0.5$ remain around $\rho \approx 0.4$ indicating the active state but those for $q = 2$ collapses into the absorbing state directly ($m = -1, \rho = 0$). When $p > p_c$, the system

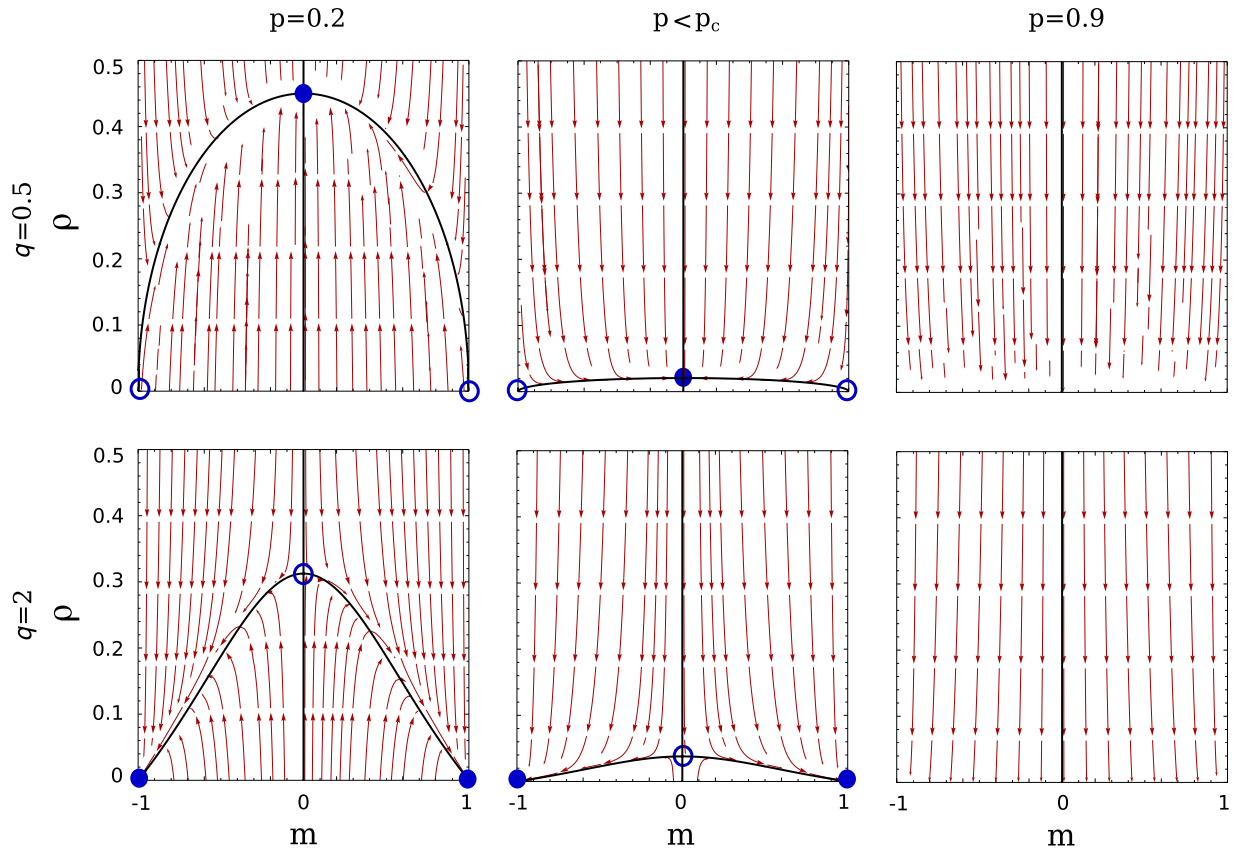


Figure 2. Flow diagram on the plane (m, ρ) for $q=0.5$ and 2 below and above $p_c=0.875$ ($q=0.5$) and 0.8 ($q=2$) obtained from pair approximation. The filled (open) circles denote the stable (unstable) fixed points. The point at $m=0$ is stable for $q=0.5$ but is unstable for $q=2$.

reaches the fragmented phase for all values of q , as shown by the green symbols (\diamond). Deviation from zero in the final state of magnetization m in a given trajectory is originated by finite size fluctuations.

The differences between a continuous or discontinuous phase transition depending on the nonlinearity are illustrated in Fig. 4 for different system sizes N . We assume that a scaling relation has a form

$$\mu = N^{\beta/\nu} f(N^{1/\nu}(p - p_c)) \tag{3}$$

where μ is a rescaled magnetization, defined as $\mu = |m|$, so that μ is 1 when the system is fully ordered either up or down and μ is zero when disordered. We find that the magnetization shows a continuous phase transition with critical exponents $\beta/\nu=0.319(1)$ for $q=0.5$ and $\beta/\nu=0.317(2)$ for $q=1$ and a diverging time to consensus at criticality. It is important here to note a singularity on the time to reach the absorbing state: while it scales linearly with $N, \tau \sim N$, for $q=1$ ¹⁷, this time increases exponentially $\tau \sim e^N$ for $q < 1$. In practice this means that for $p < p_c$ and $q < 1$ the system remains in the active dynamically state for normal observation times of a large system, at variance with the case $p=1$. For example in the trajectories shown in the right panel of Fig. 3 for $p < p_c$ in the same time scale the system has reached the absorbing state of $q=1$ but it remains around the nonzero initial value of ρ for $q=0.5$. When $q=2$, the transition becomes sharp at $p_c \approx 0.47$ as N increases and it is expected to be discontinuous in the limit $N \rightarrow \infty$. The discontinuous transition for $q=2$ is supported by non-diverging consensus time τ and the pair approximation analysis as well.

Phase diagram. We finally examine numerically the phase diagram of the system with respect to both parameters, plasticity p and degree of nonlinearity q and also the fragmentation transition when varying q . Figure 5(a) shows the phase diagram indicating consensus, coexistence, and fragmentation phases for different p and q . Typical examples of a network in each phase above and below p_c are depicted in Fig. 5(a). When $p > p_c$, the rewiring process is dominant, so the network is divided into two clusters. The two clusters are in opposite states and each cluster is in a full consensus. Therefore, when $p > p_c$, the system both for $q < 1$ and $q > 1$ reaches an absorbing state, with two oppositely ordered clusters. However, the steady state of the coevolving model below p_c relies on the degree of the nonlinearity q . If $q > 1$, all nodes belong to a single component with the same state. On the other hand, for the case $q < 1$, the system does not reach an absorbing state and remains in an active state containing both up and down nodes in the network.

By varying the degree of nonlinearity q , a discontinuous transition between consensus and coexistence phases occurs at $q=1$ for low p regime. On the other hand, as p increases, a fragmented phase appears from either the

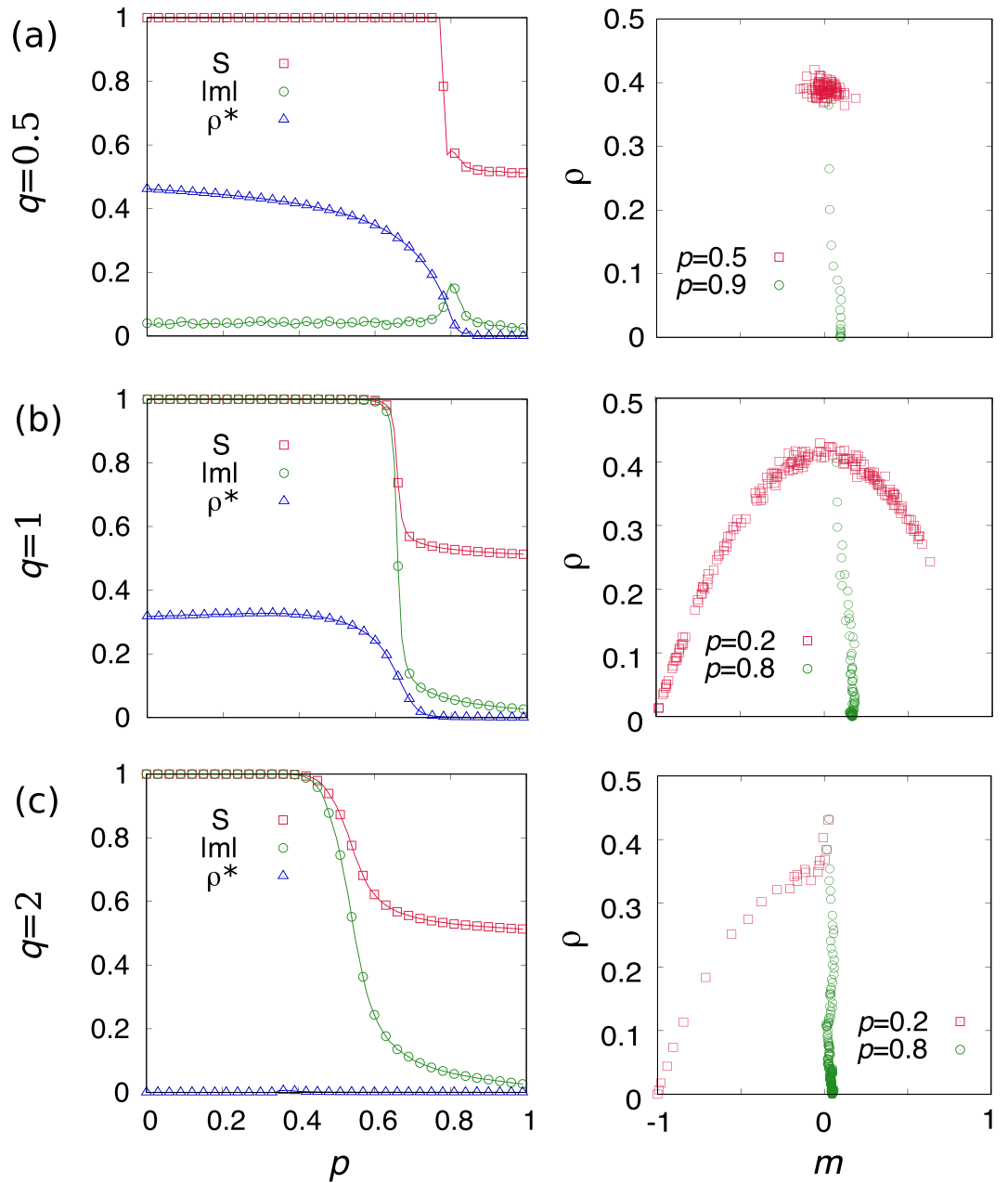


Figure 3. The size S of giant component, magnetization $|m|$, and the density ρ of active link for the network at the steady state for (a) $q=0.5$, (b) $q=1$, and (c) $q=2$ on random regular networks with $\langle k \rangle = 8$, $N = 10^3$, and initial condition $m = 0$ averaged over 10^4 realizations. The right panel represents an typical trajectory to steady state below and above p_c on (m, ρ) space.

consensus ($q > 1$) or coexistence ($q < 1$) phases. Therefore, for high enough p only the fragmented phase exists for any value of q . At intermediate values of p , three phases can be observed depending on the nonlinearity q . For example, at $p = 0.55$ we find two transitions from coexistence to consensus and subsequently from consensus to the fragmented phase as shown in Fig. 5(b). We also observe a direct transition between coexistence and fragmented phases as shown in Fig. 5(c) at $p = 0.75$. In summary, for $p < p_c(q)$ a discontinuous transition exists at $q = 1$ from a dynamically active state to a frozen absorbing state of consensus in a single component network. At $p_c(q)$ there is a fragmentation transition to an absorbing state in which the network is fragmented in two components, each of them in a different consensus state,

Discussion

In this paper, we have examined the role of nonlinearity in the coevolving voter model. We find diverse phases depending on the nonlinearity q and the rate of rewiring or plasticity parameter p . We also find that the mechanisms of network fragmentation are different for the cases $q < 1$ and $q > 1$. When $q < 1$, the system undergoes an absorbing phase transition at $p = p_c$ between one connected component in an active state and two disconnected

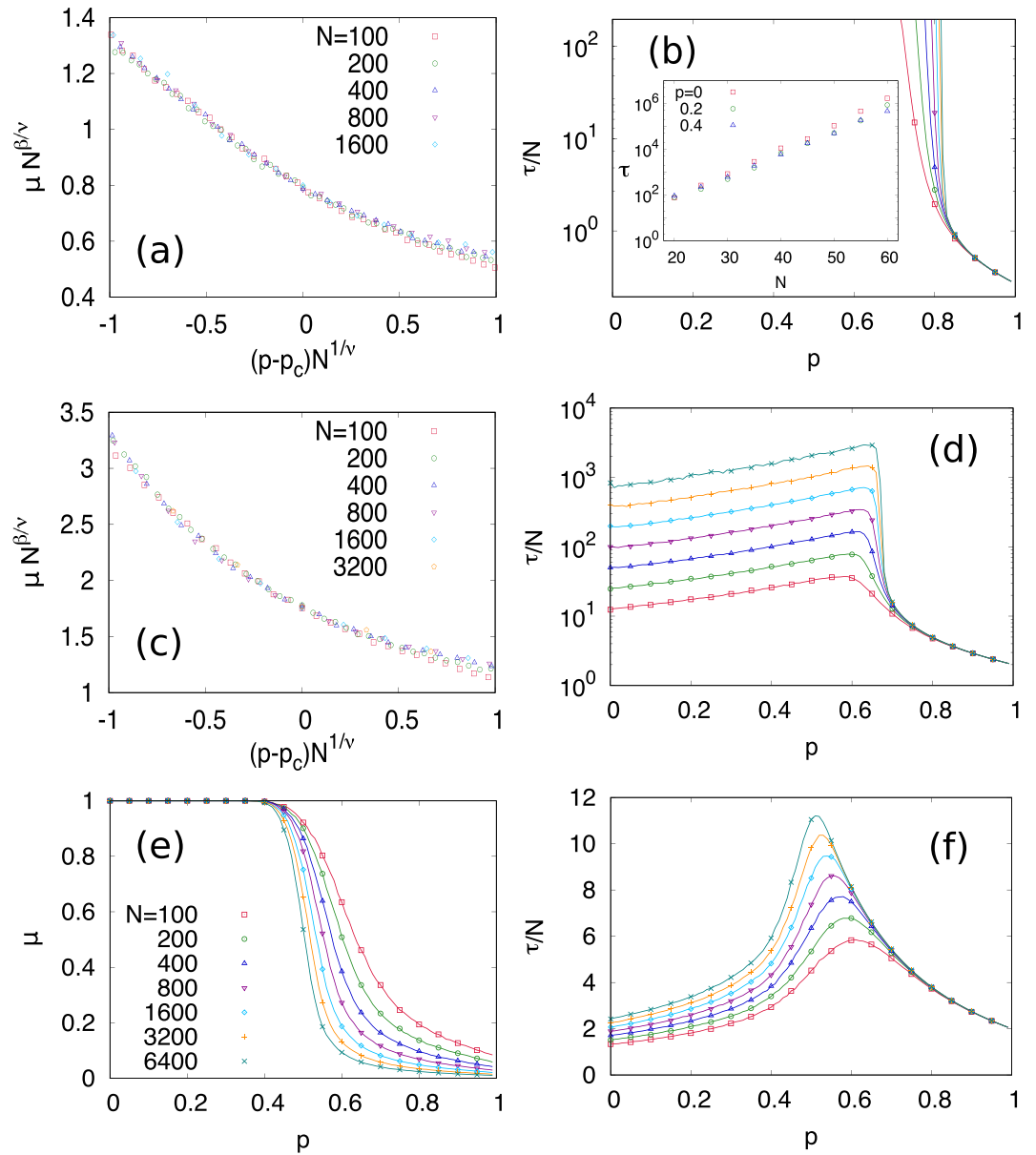


Figure 4. Rescaled magnetization μ and time to steady state τ for (a,b) $q=0.5$, (c,d) $q=1$, and (e,f) $q=2$ with different network size N and $\langle k \rangle = 8$, averaged over 10^5 runs. Figures (a) $q=0.5$ and (c) $q=1$ show scaling of magnetization in a form $\mu = N^{\beta/\nu} f(N^{1/\nu}(p - p_c))$ with $p_c \approx 0.83$ and 0.68 , respectively. When $q=0.5$, (b) τ exponentially grows with respect to N below p_c . For $q=2$, (e) the transition of magnetization is getting sharp as N increases, with (f) non-diverging τ at the transition.

clusters. In addition, the transition is continuous and characterized by the density of active links ρ vanishing at the transition point. This is the same type of transition observed for the linear voter model ($q=1$), but the time to reach the absorbing state by finite size fluctuations in the connected phase which scales linearly with N for $q=1$, scales now exponentially with N for $q < 1$. When $q > 1$, the system reaches an absorbing frozen state with $\rho=0$ for any p . For $p < p_c$, the network is in a full consensus within a single component, while for $p > p_c$ the network fragments with a discontinuous transition at $p=p_c$. This is a different type of transition to the one found in the linear voter model. Therefore, our results reveal that the nonlinearity modifies nontrivially the fragmentation transition known for the ordinary voter model ($q=1, p=p_c(q=1)$), which is a special case at the boundary between two different fragmentation transitions. In fact, three transitions lines meet in this point in the (q, p) parameter space: A continuous fragmentation transition ($q < 1, p=p_c$), a discontinuous fragmentation transition ($q > 1, p=p_c$) and an absorbing transition from an active to a frozen phase in a single component network ($q=1, p < p_c$).

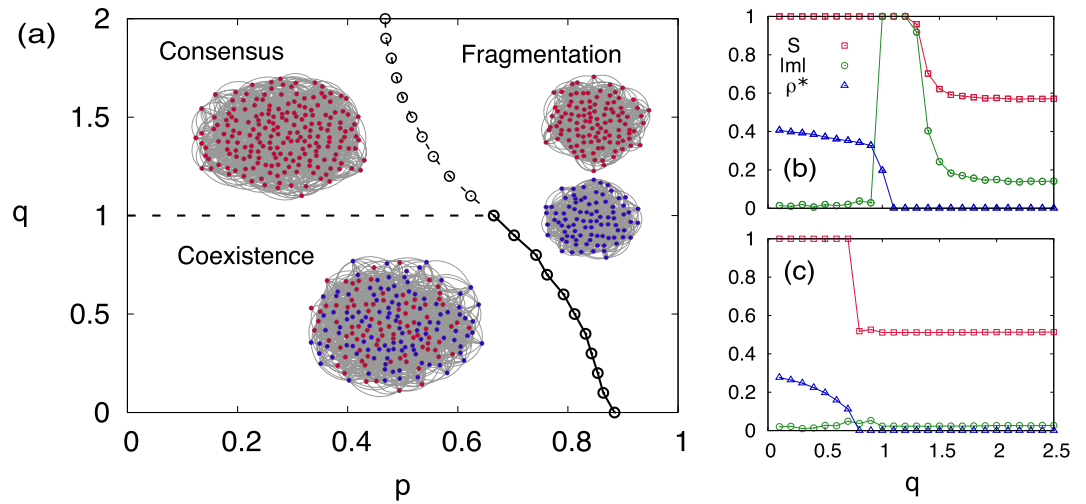


Figure 5. (a) Phase diagram with respect to p and q shows consensus, coexistence, and fragmented phases, obtained numerically on degree regular networks with $\langle k \rangle = 8$, $N = 10^4$ and initial condition $m = 0$, averaged over 10^3 realizations. Examples of network configuration at the steady-state of the coevolution model are also shown with $N = 200$ and $(p, q) = (0.2, 0.5)$ for coexistence, $(0.2, 2)$ for consensus, and $(0.8, 0.5)$ for fragmentation. Size of giant component, magnetization, and density of active links at (b) $p = 0.55$ and (c) $p = 0.75$ are also shown.

Methods

Mean-field approximation of nonlinear voter model. We first examine the nonlinear voter model on fully-connected networks where the rewiring process is not well defined, so that we take $p = 0$. A mean-field equation of the magnetization defined as $m = (1/N) \sum_i s_i$ for the fully connected networks in the limit $N \rightarrow \infty$ is simply given by

$$\frac{dm}{dt} = 2 \left[- \left(\frac{1+m}{2} \right) \left(\frac{1-m}{2} \right)^q + \left(\frac{1-m}{2} \right) \left(\frac{1+m}{2} \right)^q \right]. \quad (4)$$

Once m is given, the density of active links is determined by

$$\rho = \frac{1}{2}(1 - m^2). \quad (5)$$

There are three steady state solutions of eq. (4), $m = -1, 0$, and 1 for any q . The stability of the solutions depends on q . If $q < 1$, the neutral state $m = 0$ showing the same fraction of up and down states is stable. However if $q > 1$, the absorbing states either $m = -1$ or $m = 1$ become stable, so the system is in a fully ordered state. For $q = 1$, the magnetization m is conserved as known for the ordinary voter model.

Pair approximation of coevolving nonlinear voter model. In a random network, the density of active links ρ and the magnetization m are coupled quantities. We study their coupled evolution within a pair approximation for well mixed populations. We assume degree regular random networks. Due to the evolution of networks ($p \neq 0$), the degree regular structure is not maintained in time, but the assumption is still reasonable because an homogeneous structure is observed due to the random rewiring process. Given that we pick a node with state s , the conditional probability that we select a node connected to it, but in a different state is given by $\rho/(2n_s)$ where $s \in \{+, -\}$ and n_s represents the global fraction of nodes in s state. In addition, when we choose a node with state s to be updated with the probability $[\rho/(2n_s)]^q$, this node has approximately q neighbors in a different state. And, the other neighbors $k - q$ have a different state with probability $\rho/(2n_s)$. Putting all these together, the coupled equations for ρ and m in a mean-field pair approximation level with $N \rightarrow \infty$ ^{17,25,37,38} are:

$$\frac{dm}{dt} = 2(1 - p) \left[-n_+ \left(\frac{\rho}{2n_+} \right)^q + n_- \left(\frac{\rho}{2n_-} \right)^q \right], \quad (6)$$

$$\begin{aligned} \frac{d\rho}{dt} = \frac{2}{\langle k \rangle} & \left[-p \left[n_+ \left(\frac{\rho}{2n_+} \right)^q + n_- \left(\frac{\rho}{2n_-} \right)^q \right] + (1-p) \right. \\ & \left. \left[n_+ \left(\frac{\rho}{2n_+} \right)^q \left(\langle k \rangle - 2q - 2(\langle k \rangle - q) \frac{\rho}{2n_+} \right) \right] \right. \\ & \left. + (1-p) \left[n_- \left(\frac{\rho}{2n_-} \right)^q \left(\langle k \rangle - 2q - 2(\langle k \rangle - q) \frac{\rho}{2n_-} \right) \right] \right], \end{aligned} \quad (7)$$

where $n_+ = (1+m)/2$ and $n_- = (1-m)/2$. The steady state solutions of these equations and their stability are discussed in the main text.

References

- Boccaletti, S., Latora, V., Moreno, Y., Chavez, M. & Hwang, D. U. Complex networks: Structure and dynamics. *Physics Reports* **424**, 175–308 (2006).
- Barrat, A., Barthelemy, M. & Vespignani, A. Dynamical processes on complex networks. (Cambridge university press, 2008).
- Barabási, A.-L. & Albert, R. Emergence of scaling in random networks. *Science* **286**, 5439 (1999).
- McPherson, J. M., Smith-Lovin, L. & Cook, J. Birds of a feather: Homophily in social networks. *Ann. Rev. Sociol.* **27**, 415–444 (2001).
- Centola, D., González-Avella, J. C., Eguíluz, V. M. & San Miguel, M. Homophily, cultural drift, and the co-evolution of cultural groups. *J. of Conflict Resol.* **51**, 905 (2007).
- Min, B., Liljeros, F. & Makse, H. A. Finding influential spreaders from human activity beyond network location. *PLoS ONE* **10**, e0136831 (2015).
- Zimmerman, M. G., Eguíluz, V. M. & San Miguel, M. Cooperation, adaptation and the emergence of leadership. Lecture Notes in Economics and Mathematical Series, Vol. 503, edited by Kirman, A. & Zimmermann, J.-B. pp. 73–86 (Springer, 2001).
- Gross, T. & Blasius, B. Adaptive coevolutionary networks: a review. *J. Royal Soc. Interface* **5**, 259–271 (2008).
- Gross, T. & Sayama, H. *Adaptive Networks*. (Springer, Heidelberg, 2009).
- Zimmerman, M. G., Eguíluz, V. M. & San Miguel, M. Coevolution of dynamical states and interactions on networks. *Phys. Rev. E* **69**, 065102 (2004).
- Pacheco, J. M., Traulsen, A. & Nowak, M. A. Coevolution of strategy and structure in complex networks with dynamical linking. *Phys. Rev. Lett.* **97**, 258103 (2006).
- Szolnoki, A., Perc, M. & Danku, Z. Making new connections towards cooperation in the prisoner's dilemma game. *EPL (Europhysics Letters)* **84**, 50007 (2008).
- Perc, M. & Szolnoki, A. Coevolutionary game - a mini review. *BioSystems* **99**, 109–125 (2010).
- Wang, Z., Szolnoki, A. & Perc, M. Self-organization towards optimally interdependent networks by means of coevolution. *New J. Phys.* **16**, 033041 (2014).
- Holme, P. & Newman, M. E. J. Nonequilibrium phase transition in the coevolution of networks and opinions. *Phys. Rev. E* **74**, 056108 (2006).
- Vazquez, F., González-Avella, J. C., Eguíluz, V. M. & San Miguel, M. Time scale competition leading to fragmentation and recombination transitions in the co-evolution of network and states. *Phys. Rev. E* **76**, 046120 (2007).
- Vazquez, F., Eguíluz, V. M. & San Miguel, M. Generic absorbing transition in coevolution dynamics. *Phys. Rev. Lett.* **100**, 108702 (2008).
- Herrera, J. L., Cosenza, M. G., Tucci, K. & González-Avella, J. C. General coevolution of topology and dynamics in networks. *EPL (Europhysics Letters)* **95**, 58006 (2011).
- Gross, T., D'Lima, C. J. D. & Blasius, B. Epidemic dynamics on an adaptive network. *Phys. Rev. Lett.* **96**, 20 (2006).
- Gross, T. & Sayama, H. eds, *Adaptive Networks: Theory, Models, and Data* (Springer, 2009).
- Scarpino, S. V., Allard, A. & Hébert-Dufresne, L. The effect of a prudent adaptive behaviour on disease transmission. *Nat. Phys.* **12**, 1042–1046 (2016).
- Kimura, D. & Hayakawa, Y. Coevolutionary networks with homophily and heterophily. *Phys. Rev. E* **78**, 016103 (2008).
- Böhme, G. & Gross, T. Analytical calculation of fragmentation transitions in adaptive networks. *Phys. Rev. E* **83**, 035101(R) (2011).
- Durrett, R. *et al.* Graph fission in an evolving voter model. *Proc. Natl. Acad. Sci. USA* **109**, 3682 (2012).
- Demirel, G., Vazquez, F., Böhme, G. & Gross, T. Moment-closure approximations for discrete adaptive networks. *Physica D* **267**, 68 (2014).
- Diakonova, M., San Miguel, M. & Eguíluz, V. M. Absorbing and shattered fragmentation transitions in multilayer coevolution. *Phys. Rev. E* **89**, 06218 (2014).
- Diakonova, M., Eguíluz, V. M. & San Miguel, M. Noise in coevolving networks. *Phys. Rev. E* **92**, 032803 (2015).
- Klimek, P. *et al.* Dynamical origins of the community structure of an online multi-layer society. *New J. Phys.* **18**, 083045 (2016).
- Castellano, C., Muñoz, M. A. & Pastor-Satorras, R. Nonlinear q -voter model. *Phys. Rev. E* **80**, 041129 (2009).
- Schweitzer, F. & Behera, L. Nonlinear voter models: the transition from invasion to coexistence. *Eur. Phys. J. B.* **67**, 301–318 (2009).
- Centola, D., Eguíluz, V. M. & Macy, M. W. Cascade dynamics of complex propagation. *Physica A* **374**, 449 (2007).
- Czaplicka, A., Toral, R. & San Miguel, M. Competition of simple and complex adoption on interdependent networks. *Phys. Rev. E* **94**, 062301 (2016).
- Nowak, A., Szamrej, J. & Latané, B. From private attitude to public opinion: A dynamic theory of social impact. *Psychological Review* **97**, 362 (1990).
- Abrams, D. M. & Strogatz, S. H. Linguistics: Modelling the dynamics of language death. *Nature* **424**, 900 (2003).
- Vazquez, F., Castello, X. & San Miguel, M. Agent based models of language competition: macroscopic descriptions and order-disorder transitions. *J. Stat. Mech.* **04**, P04007 (2010).
- Nettle, D. Using social impact theory to simulate language change. *Lingua* **108**, 95 (1999).
- Vazquez, F. & Eguíluz, V. M. Analytical solution of the voter model on uncorrelated networks. *New J. Phys.* **10**, 063011 (2008).
- Jedrzejewski, A. Pair approximation for the q -voter model with independence on complex networks. *Phys. Rev. E* **95**, 012307 (2017).

Acknowledgements

We thank M. Cosenza for useful discussions. This work was supported by the Spanish Ministry MINEiCO and FEDER (EU) under the project ESOTECOS (FIS2015-63628-C2-2-R).

Author Contributions

All authors conceived the study, performed the research, analyzed data, and wrote the paper.

Additional Information

Competing Interests: The authors declare that they have no competing interests.

Publisher's note: Springer Nature remains neutral with regard to jurisdictional claims in published maps and institutional affiliations.



Open Access This article is licensed under a Creative Commons Attribution 4.0 International License, which permits use, sharing, adaptation, distribution and reproduction in any medium or format, as long as you give appropriate credit to the original author(s) and the source, provide a link to the Creative Commons license, and indicate if changes were made. The images or other third party material in this article are included in the article's Creative Commons license, unless indicated otherwise in a credit line to the material. If material is not included in the article's Creative Commons license and your intended use is not permitted by statutory regulation or exceeds the permitted use, you will need to obtain permission directly from the copyright holder. To view a copy of this license, visit <http://creativecommons.org/licenses/by/4.0/>.

© The Author(s) 2017